forests

MDPI

Review

A Review of General Methods for Quantifying and Estimating Urban Trees and Biomass

Mingxia Yang [1], Xiaolu Zhou [1], Zelin Liu [1], Peng Li [1], Jiayi Tang [1], Binggeng Xie [1] and Changhui Peng [1,2,*]

[1] School of Geographic Sciences, Hunan Normal University, Changsha 410081, China; yangmx9495@163.com (M.Y.); zhoux1977@163.com (X.Z.); zelin.liu@hunnu.edu.cn (Z.L.); lipeng2019@hunnu.edu.cn (P.L.); tangjiayi24@hunnu.edu.cn (J.T.); xbgyb1961@163.com (B.X.)

[2] Department of Biology Sciences, Institute of Environment Sciences, University of Quebec at Montreal, Case Postale 8888, Succursale Centre-Ville, Montreal, QC H3C 3P8, Canada

* Correspondence: peng.changhui@uqam.ca

Abstract: Understanding the biomass, characteristics, and carbon sequestration of urban forests is crucial for maintaining and improving the quality of life and ensuring sustainable urban planning. Approaches to urban forest management have been incorporated into interdisciplinary, multifunctional, and technical efforts. In this review, we evaluate recent developments in urban forest research methods, compare the accuracy and efficiency of different methods, and identify emerging themes in urban forest assessment. This review focuses on urban forest biomass estimation and individual tree feature detection, showing that the rapid development of remote sensing technology and applications in recent years has greatly benefited the study of forest dynamics. Included in the review are light detection and ranging-based techniques for estimating urban forest biomass, deep learning algorithms that can extract tree crowns and identify tree species, methods for measuring large canopies using unmanned aerial vehicles to estimate forest structure, and approaches for capturing street tree information using street view images. Conventional methods based on field measurements are highly beneficial for accurately recording species-specific characteristics. There is an urgent need to combine multi-scale and spatiotemporal methods to improve urban forest detection at different scales.

Keywords: biomass model; forest carbon; individual tree; tree biomass; tree model; urban forest

Citation: Yang, M.; Zhou, X.; Liu, Z.; Li, P.; Tang, J.; Xie, B.; Peng, C. A Review of General Methods for Quantifying and Estimating Urban Trees and Biomass. *Forests* **2022**, *13*, 616. https://doi.org/10.3390/f13040616

Academic Editors: Ram P. Sharma and Xiangdong Lei

Received: 4 March 2022
Accepted: 11 April 2022
Published: 15 April 2022

1. Introduction

Rapid urbanization has become one of the most characteristic modern phenomena globally, causing changes to society, the economy, and the environment [1]. In 2018, 55% of the world's population resided in urban areas, and by 2050, the percentage is projected to increase to 68% (UN DESA 2018). This unprecedented urbanization has profoundly shaped urban ecosystems, leading to fragmented landscapes and the disturbance of biodiversity and biogeochemical cycles. It is estimated that the carbon released by human activities in cities accounts for approximately 71% of global energy-related carbon dioxide emissions (World Energy Outlook, 2018). Furthermore, rapid urbanization has led to changes in the environment, including a reduction in biodiversity [2], deterioration of air quality [3,4], and a decrease in the amount of green space [5,6]. As urbanization continues, understanding and quantifying the provision of ecosystem services within cities, especially the demand for carbon sequestration capacity, will help to address environmental and social challenges [7].

Urban forests, including individual trees, forest stands, and related biological and environmental elements, are regarded as carbon sinks [8]. The characteristics, functions, and structures of trees provide diverse benefits and ecosystem services that can mitigate the adverse effects of urbanization [9]. Biomass factors can reflect whether a forest ecosystem has healthy environmental conditions [10]. Therefore, carbon sequestration in urban trees can be assessed by estimating and quantifying biomass. Currently, the loss of forest biomass in urban areas has become a focus of global attention [11]. As a result, urban ecosystem

function has increasingly required accurate forest biomass estimation and structural dynamics detection [12]. Therefore, the investigation of urban forest biomass enables a better understanding of the relationship between urban trees and global carbon emissions and consequently improves urban planning and management.

A wealth of information regarding individual trees can improve our ability to estimate forest biomass and provide tree-level details for urban ecological research [13]. Urban forests are mosaics of different ages and species and usually have high spatial heterogeneity [14]. Therefore, it is necessary to extract individual urban trees and capture their attributes, including their morphological features (e.g., leaf area and diameter at breast height (DBH)) and structure (e.g., species composition and spatial pattern) [15]. These attributes of individual trees have been widely used in various studies, such as monitoring the growth and health of trees and providing basic data for three-dimensional modeling of trees [16–18]. This information is usually collected using conventional technology and relies on allometric equations and field measurements of species distributions [12]. Remote sensing images are frequently applied in biomass mapping and the extraction of vegetation characteristics in urban environments [19]. Urban forests have been described in greater detail because of improvements in technological capabilities. Recently, the rapid development of machine learning techniques and big data applications has enabled street view images to provide unprecedented opportunities for urban forest investigations [20–22].

With recent developments in urban forest research and the establishment of its key role in global science, it is necessary to synthesize and update the latest developments in this field. This review provides a systematic review of the advances in urban forest research methods. We focused on estimating urban forest biomass and identifying individual trees using different approaches. We discuss in detail the achievements, challenges, and opportunities presented by different methods in identifying the characteristics and dynamics of urban forests and their influences on the monitoring and evaluation of urban forests in the context of global change.

2. Estimation Methods for Urban Forest Biomass

To mitigate the risk of climate change, a comprehensive understanding of carbon sequestration is required [23]. Different approaches can be considered to estimate forest biomass, namely: (i) field-based measurements and biomass allometric growth equations; and (ii) remote-based inventories. Combining methods based on different measurement principles is often more efficient for quantifying carbon storage and urban forest sequestration [24] (Figure 1).

2.1. Field-Based Inventory

Field sampling and data measurements are the most conventional yet highly beneficial methods for estimating urban forest biomass, providing direct first-hand evidence of urban forest dynamics. Destructive sampling requires direct measurement and nondestructive sampling which involves the application of allometric equations [25]. The direct method is usually performed by physically weighing tree components [26]. This method is limited to small areas or small tree sample sizes. This method accurately determines biomass in a specific region and is time-consuming, destructive, and costly. Therefore, it is not suitable for non-commercial forestry in urban areas [12]. Typically, this method is used to develop biomass equations for large scale biomass quantification [27].

Indirect methods involve establishing allometric equations for carbon estimation in urban forests [28,29]. Allometric equations allow the calculation of biomass using tree sizes. Tree species, wood density, tree height, tree volume, and DBH have been used to estimate forest biomass [30]. Biomass estimation at the city and landscape level based on field inventories mainly involves three steps: (1) selection of allometric biomass equations for individual tree biomass estimation, (2) accumulation of single-tree biomass for estimating sample plot biomass, and (3) calculation of biomass at the landscape level based on the average values of the sample plots. The selection of equations may affect

biomass estimation in urban forests. Applying forest-based equations to tree species is inferior to using urban-based equations [31]. Specific urban environments may increase biomass variation depending on various factors, such as species, scale, allometric equations, population, and community characteristics [12]. Species-specific equations are usually preferred when a more precise estimation of the volume and biomass of specific trees and forest types is required, such as for high-value species or environmental management purposes [12,32]. However, the limitations of these species-specific equations stem from the cost of biomass measurement, which is generally based on small-scale projects due to destructive sampling difficulties in urban environments [33].

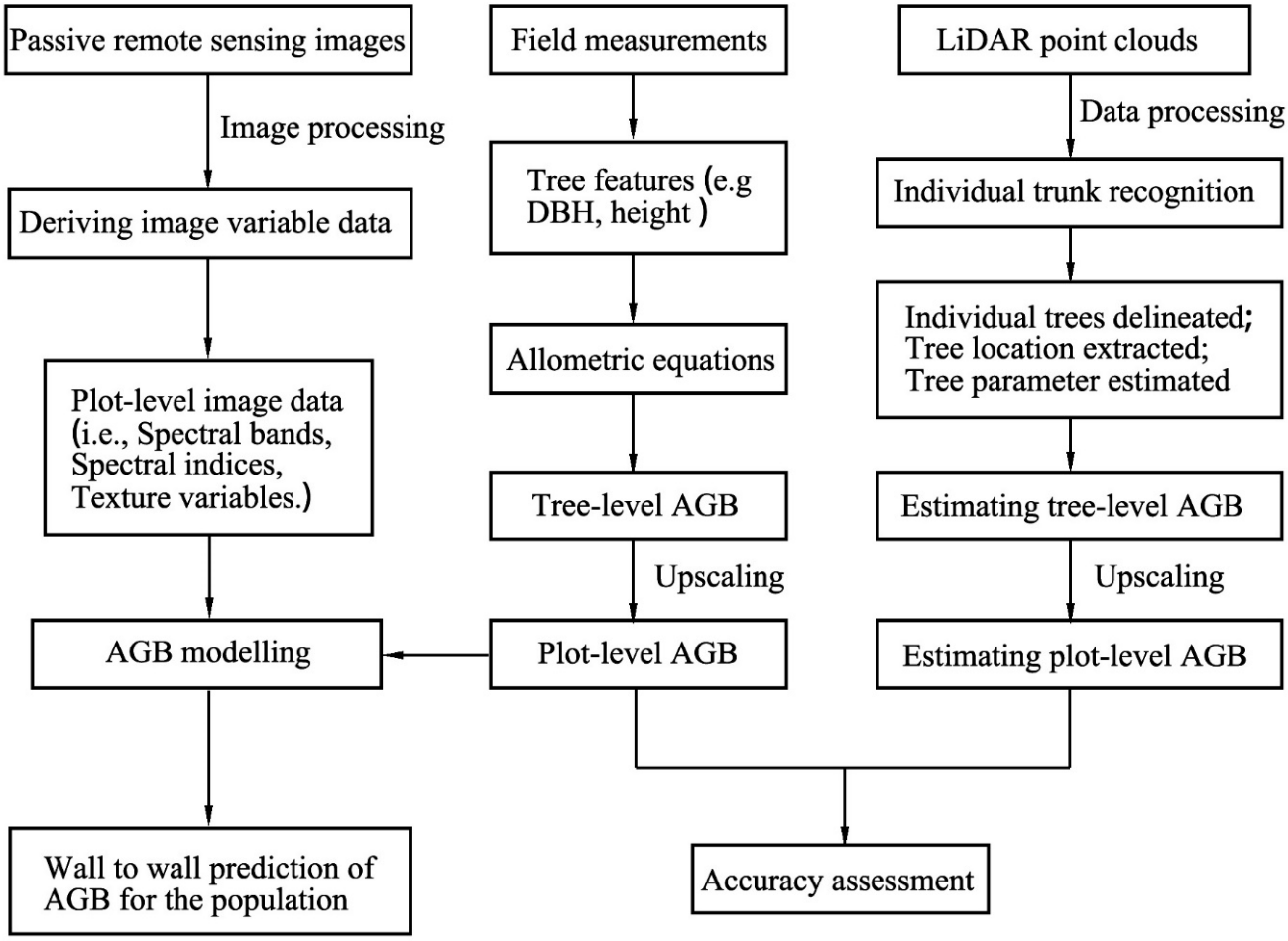

Figure 1. Framework for a system of integrated field measurements, passive remote sensing images, and LiDAR point clouds to extract tree attributes and aboveground biomass. LiDAR: light detection and ranging; AGB: aboveground biomass; DBH: diameter at breast height.

In summary, urban forest biomass estimation may require more methods and allometric equations that apply to urban environments. Considering the time and monetary cost of developing species-specific allometric equations, more research is required to develop general allometric equations to detect urban trees. Existing models to quantify the biomass and carbon dynamics of urban trees are based on generalized allometric biomass equations and mainly rely on cross-sectional data of urban or natural forests in most temperate and northern cities [8,26]. Nowak and Crane updated urban general allometric equations based on data from eight new cities to quantify the carbon storage of urban trees and tree coverage data [34]. The advantage of these equations is that the relationship between tree characteristics and biomass can be developed with fewer trees and applied to other trees of similar shapes [35].

Notably, the potential error in applying general allometric equations developed for natural trees could be substantial when directly used in urban forests. The general equations overestimated the number of open-grown urban forests [36]. The carbon storage of urban forests was estimated using forestland biomass allometric equations multiplied by a correction factor of 0.8 [34]. The standard application of the correction factor may lead to an underestimation of urban forest biomass. Applying a 20% reduction to the biomass estimation of street trees, the estimate was 30% lower than the field-based measurements in urban street areas [12]. Another study established a general equation for urban broadleaf species that overestimated aboveground biomass (AGB) by 50% [37]. Although correction factors have been widely used in urban forestry research, there is limited evidence to validate or support their value. The differences between species structures used to generate general urban equations and urban tree populations may be the cause of this situation [30].

The selection of an appropriate allometric biomass equation is one of the greatest sources of uncertainty, depending on multiple factors, such as species composition and plot size [38,39]. Furthermore, allometric models are usually only fitted with a limited number of trees and species and might not be representative of a regional tree species pool [40]. In addition, different climatic conditions can affect urban growth, and the equations for specific species lack accuracy or universal applicability, which might affect large-scale estimates [41]. Therefore, an allometric equation should be carefully selected to estimate urban forest carbon.

2.2. Remote Sensing-Based Approach

2.2.1. Passive Optical Remote Sensing

Remote sensing techniques provide approaches for collecting data on forest distribution and structure, while avoiding many of the challenges of conventional methods [42]. A wide range of remote sensing approaches employ single or multiple sensors, and passive or active remotely sensed data have been increasingly employed to investigate forest cover changes and estimate carbon storage [43,44]. Passive optical satellite images can provide information on the uppermost characteristics of a forest, and AGB can be obtained indirectly through empirical relationships between spectral indices or reflectance and canopy parameters [45,46]. A wide range of remote sensing methods for AGB estimation has been derived, from low-resolution (e.g., MODIS, Landsat, and ASTER) to very high-spatial resolution (e.g., Quickbird, IKONOS, and WorldView) remote sensing imaging.

Multispectral remote sensing images from (coarse resolution, 200–1000 m; medium resolution, 20–30 m) satellite platforms have gained in popularity when it comes to obtaining comprehensive spatial information on forest characteristics over large areas. In particular, sensors for Landsat missions are usually based on regression models of surface reflectance bands, derivative vegetation indices, and image transformations to map urban forest biomass and dynamics [45,47]. The Landsat Thematic Mapper (TM) and the Enhanced Thematic Mapper (ETM+) have become the most common approaches for depicting the spatiotemporal distribution of forest structure, as data with a spatial resolution of 30 m can be obtained for free [48,49]. Although these medium- and coarse-resolution datasets lack the detailed information required to map urban vegetation accurately, researchers have developed many approaches based on these datasets [50,51].

Currently, very high-resolution (VHR) images are becoming increasingly relevant for urban forest observations and monitoring [52,53]. VHR images can accurately measure the height, crown diameter, and volume of trees, and estimate biomass through allometric relationships [54,55]. VHR data have been used to map urban vegetation in many cities worldwide, including Hong Kong [56], Vancouver [57], and Los Angeles [58]. However, most VHR images are confined to a small area for a short period due to the high costs and limited availability in urban areas, thus limiting their usefulness in urban planning. In summary, exploring the relationship between spectral traits (coarse, medium, and VHR) and urban forest carbon storage is challenging. As passive sensors mainly explore the upper crown in a two-dimensional structure, it is not easy to detect the vertical structure

of the forest for estimating AGB and carbon storage [45]. Furthermore, the availability of multispectral satellite data is limited by the inability to classify cloud-covered areas [59].

2.2.2. Light Detection and Ranging

The development of Light Detection and Ranging (LiDAR) has led to breakthroughs in forest resource inventory [60,61]. The LiDAR system detects horizontal and vertical distances between the sensor and the target, providing data to generate a three-dimensional forest structure (e.g., canopy height, coverage, and volume) that can be further used to infer forest biomass [62,63]. The connection between such systems and urban forest resource inventories can be regularly exploited to determine the structure and function of urban forests [64] and to estimate the biophysical parameters of individual urban trees [65], predict the regional AGB of forests [66], and quantify forest carbon dynamics [67]. In addition, LiDAR methods achieve a lower uncertainty in estimating AGB at different spatial scales because of the stronger correlation between biomass and tree height [68].

Various studies have reported the successful use of airborne laser scanning (ALS), terrestrial laser scanning (TLS), and mobile laser scanning (MLS) for biomass estimation and 3D structure measurements at the individual tree level [69–71] (Figure 2). ALS data have been widely applied to detect individual tree crowns at large scales among these three technologies [72,73]. Focusing on the urban environment, the results of the Vancouver case study demonstrated that large individual canopies could be mapped with an ALS point cloud-derived raster and an object-based workflow [74]. The application of high-density ALS data has also proven its potential in the fully automated classification of urban coniferous or deciduous forests [75,76]. However, given the complexity and heterogeneity of forest structure and composition, ALS may not capture the complete vertical distribution of a crown [77]. Recently, TLS techniques have been used as a complementary approach to ALS [78]. They allow DBH, stem density, and crown shape to be obtained by providing a considerable amount of precise information about various forest structure parameters [79,80]. ALS fills this gap in manual measurements and is more suitable for measuring millimeter-level information, from individual trees to sample plots. Methods using TLS unique distance information are more effective for estimating the leaf area of individual trees in urban areas [81,82]. The explosive increase in TLS data is revolutionizing the development of methods for automatically calculating individual tree attributes. MLS allows for the quick and cost-effective acquisition of close-range 3D measurements of street objects as part of a new mapping system [83,84]. It obtains higher point density data and more complete data coverage than the ALS system and performs more efficiently than TLS [17]. Algorithms combining MLS with digital images or videos have been successfully applied to individual tree detection with geometric parameters [85]. MLS has the potential to extract information simultaneously and automatically about roadside trees, which is promising for urban forest management [71].

Approaches that apply LiDAR to mapping urban forest biomass are associated with some uncertainties. These approaches improve data acquisition and provide a higher point density for estimating AGB. However, this may greatly increase the cost and pose a challenge to procuring and processing large volumes of LiDAR data cost-effectively for large-area assessments [86]. In addition, LiDAR pulses may miss actual treetops, and tree height estimation based on LiDAR tends to be underestimated. Owing to the lack of model generalization, this technique can only be applied to specific sites [87,88]. More effort is needed in urban forest biomass estimation to establish LiDAR-based models that are cost-effective and suitable for reasonable estimation of tree allometry.

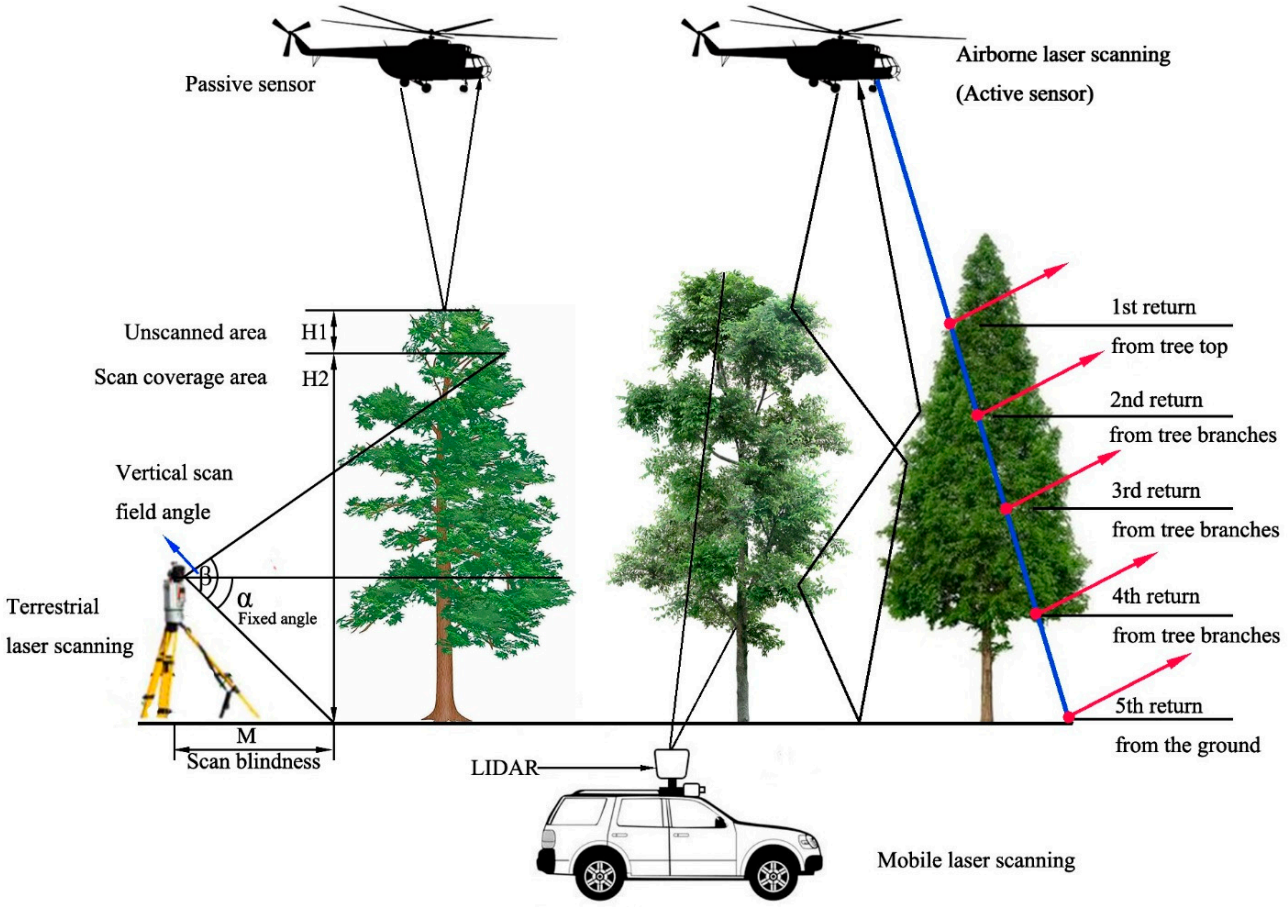

Figure 2. Data acquisition principles of airborne laser scanning (ALS), terrestrial laser scanning (TLS), and mobile laser scanning (MLS) on urban forests. The red arrows represent multiple returns from a single laser pulse.

2.2.3. Unmanned Aerial Vehicle-Based Techniques

The advent of unmanned aerial vehicles (UAVs) in forest research has provided a new method for estimating urban forest biomass and characterizing individual trees [89]. The technology offers a series of potential advantages, including high-intensity data collection, user-defined spatial and temporal resolution, and flexibility regarding the type of onboard sensor used [90]. UAVs are also particularly beneficial for investigating optical remote sensing time-series data in areas that encounter frequent cloud coverage [91]. Compared with field surveys, high-spatial resolution UAV images can capture details of ground objects to help better model biomass [90,92]. The details also allow for the classification of individual trees into deciduous and coniferous trees and the identification of specific tree species in urban areas [93]. These methods are highly attractive for urban forest assessment and provide comprehensive insights into ecosystem functions at multiple scales. The UAV method has shown great application potential for forest biomass estimation in urban areas, but some limitations still need to be addressed. For example, distinguishing trees and background objects in forest UAV images is difficult because of the large amounts of variation in terms of foreshortening, illumination, different color shades, and non-homogenous bark textures [94]. Another limitation is that the UAV method only measures the canopy from an aerial view, which can increase error if there is too much overlap between individual trees [95]. These challenges remain unresolved.

3. Estimation and Identification of Individual Trees

Extracting forest structure information at the individual tree level is critical for many forest managements and ecology applications [96]. The characteristics of individual trees are also valuable in estimating forest biomass and updating forest inventories [97]. In addition, deriving a register of the attributes (e.g., species, DBH, tree distribution, stem volume, and biomass) of individual trees is beneficial for establishing maintenance actions [98]. Urban forest models, machine learning methods, and detection methods based on street view images are promising techniques for estimating and identifying individual urban trees.

3.1. Urban Forest Models

Unlike some simple empirical models used in conventional estimations, comprehensive urban forest models can quantify the benefits of street trees and explain differences in tree type and size. This type of model is a roadside tree-specific analysis tool for urban forest managers that uses forest inventory data to quantify structures, functions, and ecosystem services [99,100]. For example, i-Tree, ENVI-met, computational fluid dynamic, and CITYgreen models are widely used to detect and estimate urban forests [101,102]. One of these models, i-Tree (www.itreetools.org) accessed on 2 February 2022, is a software suite developed by the United States Department of Agriculture (USDA) Forest Services that helps researchers and managers estimate the structure and ecological functions of urban forests [103]. Two sub-models in the i-Tree toolset, i-Tree Streets (formerly UFORE) and i-Tree Eco (formerly STRATUM), estimate the magnitude of ecosystem services from average growth rates, biomass allometry equations, and the canopy features of different species. The i-Tree model successfully compared the forest carbon stocks of 14 cities in the United States, suggesting that the model provides valuable insights into tree populations, total carbon storage, gross and net carbon sequestration, and the sustainability of urban forests [104]. Although urban forest carbon estimation models based on the i-Tree tool have shown high effectiveness in monitoring carbon dynamics across cities, their uncertainties cannot be ignored [105]. For example, in the i-Tree model, only sampling errors with field map data were evaluated, and errors due to model structure and parameters are not taken into account, leading to uncertainty in the estimation of urban forest biomass [8].

3.2. Deep Learning Techniques

Machine learning techniques have become powerful tools in the remote sensing community because of their outstanding performance in terms of model versatility and accuracy. Machine learning techniques have advanced and introduced new methods for the most common remote sensing processing tasks, such as classification, change detection, image processing, and accuracy assessment. Machine learning combined with object-based image analysis techniques has been well established for recognizing and detecting objects in red–green–blue (RGB) images. Deep learning, a branch of machine learning, has created computationally efficient relational models in remote sensing [106]. It is particularly suitable for the image interpretation and pattern recognition of spatial data using convolutional neural networks (CNN) [107]. Due to its superiority in high-level feature representation and scene identification, CNN has demonstrated great potential for urban forest estimation and identification at the individual tree level. In deep learning applications, individual tree crown detection and species classification are common research topics in deep learning [108,109]. From the perspective of crown detection, deep learning methods based on RGB and LiDAR data can be used to identify individual trees. CNN can be used to classify dominant tree species in highly complex urban environments [110]. Furthermore, CNN-based object detectors can classify and list the geographic locations of roadside trees from street views and aerial images [111,112].

Presently, deep learning still has limitations in practical tree detection. Lack of training data is a common problem in deep learning owing to the high cost of data collection and annotation [81]. For tree detection, high variability in canopy appearance increases the

risk of overfitting when using small amounts of a training dataset owing to taxonomy, health status, and human management [113]. The challenge for individual tree crown detection and tree species classification based on deep learning is the seasonal foliage variation of deciduous trees, which may limit the generalization of the classification [22]. Generally, deep learning can provide more accurate results than conventional or shallow neural network methods when a large amount of data is available [114,115].

3.3. Urban Tree Detection Based on Street View Images

Street view images provide a new opportunity for fine-scale urban ecology research from a ground-level perspective [116]. With this approach, numerous roadside tree photos are acquired which can be processed using deep learning or manual interpretation methods to generate rich information about street trees, such as DBH, tree height, and tree species [112,117] (Figure 3). For example, street view images can be used to estimate the impact of tree shadows [118], access to forest coverage, and urban parks [119] and evaluate the relationship between distributions of vegetation in different cities [113]. These urban forest factors visually reflect the amount of vegetation seen from the perspective of pedestrians. These can be quantified using a hierarchical model based on street view images [120]. This tree census method, which does not require manual field surveys or time-consuming processing, demonstrates a large-scale and high-speed urban tree investigation approach using geographically extensive and freely available data sources [117,121]. There are weaknesses associated with the use of street view images, most notably that coverage is limited to street landscapes. Street view images are not available in areas where roads are sparse and within most large open spaces, such as parks and conservation lands [122]. Overall, street view imaging is cost-effective, efficient, and highly feasible for field inventory data collection to obtain information on street trees.

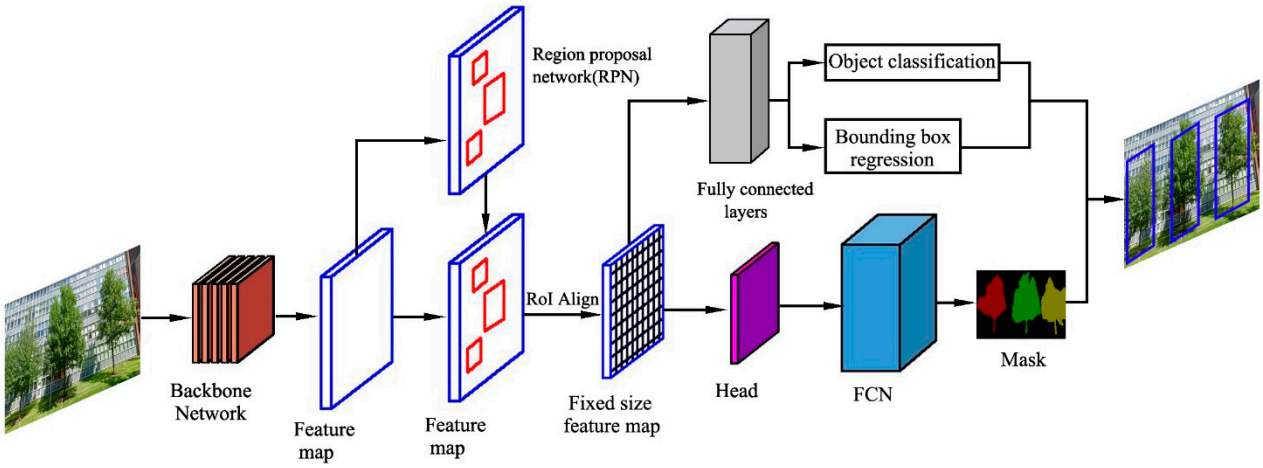

Figure 3. Urban tree detection based on Mask R-CNN and Google Street View imaging. Backbone Network refers to the image as input and extracts "feature maps"; RPN generates the proposal for object detection; RoI (region of interest) is a proposed region from the original image. RoI Align is an operation for extracting a small "feature map" from each RoI in detection and segmentation. FCN represents a fully convolutional network.

4. Discussion

4.1. Field-Based vs. Remote Sensing-Based Approaches

For field-based and remote sensing data approaches, trade-offs exist in terms of accuracy, coverage, and cost-effectiveness, depending on the type of data required to achieve the research goals (Table 1). Trade-offs include collecting sufficient field measurement data to provide records of forest attributes at different spatial scales and continuously across broad geographic areas. Field-based methods are highly accurate. However, the major challenge

in collecting data to assess forest stand conditions is that these methods are labor-intensive, time-consuming, spatially restricted, difficult to access, and extremely destructive [123]. In addition, these measurements are very expensive and are usually interpolated from relatively small field plots to obtain information for a large geographic area [124]. The interpolation of data based on a small number of plots can lead to significant uncertainties when assessing large carbon storage areas and complex forest structures [125,126].

Table 1. Strengths and weaknesses of forest biomass estimation and tree detection methods.

Methods	Strengths	Weaknesses (Limitations)	References
1. Forest biomass			
(1). Field-based inventory	Highly accurate; abundant indicators available	Time and resource consuming; labor-intensive, destructive, and expensive; limited to small areas and small tree sample size	[12,25,33]
(2). Remote sensing-based approach	Cost-effective; data spatially explicit and continuous; data available at multiple temporal and spatial scales	Difficult to obtain forest structure information; limited by biomass models; highly uncertainty	[10,127]
2. Tree detection			
(1). Urban forest models	Accurate to the individual plant scale; simplified and generalized operation	Model structure and parametric uncertainties	[105]
(2). Deep learning	More effective for urban tree species classification; flexibility and accuracy	Lack of training data; the cost of data collection and annotation; difficulty to obtain the ground truth information	[114,128,129]
(3). Street view image-based technique	A very fine level from the ground perspective; freely available, geographically extensive data sources; cost-effective, high efficiency, and strong feasibility	Not available where road access is sparse, within most large open spaces; limited to streetscapes	[117,121,122]

Conversely, remote sensing techniques can overcome the limitations of field-based observations and have the potential to provide cost-effective, continuous, and spatially explicit data at multiple temporal and spatial scales (Figure 1) [127]. Additionally, remote sensing data can provide information that may not be easily measured in the field, such as landscape metrics and retrospective change detection monitoring [130]. However, remote sensing techniques can only assess trees visible in the sky, making it difficult to capture details of tree species composition, diversity, and forest structure. Urban forest remote sensing detection techniques face uncertainties owing to structural variation, landscape heterogeneity, seasonal variation, and disproportionate data availability [10,131]. Although field measurement methods are still insufficient for the regular sampling of large or inaccessible areas, monitoring methods that combine field and remote sensing can provide efficient solutions to forest management challenges.

Considering these analyses, field-based and remote sensing methods can complement each other when exploring fragmented urban forests. Remote sensing can be used to map tree species composition and forest attributes in a landscape, whereas field-based measurements can be used to obtain relatively accurate characteristics and validate remote sensing data [132,133]. da Cunha Neto et al. [134] used UAV-LiDAR to derive the individual tree heights of pine trees in a city, the results of which were highly correlated with field-based data. Therefore, it is advantageous to combine field and remote sensing data to explore the structure and attributes of urban forests.

4.2. Remote Sensing-Based Techniques: A Matter of a Trade-Off?

Increasingly, remote sensing data can be used in forest surveys to map the features of forest crown coverage, forest constitutions, and dynamics [135]. Remote sensing images can be generated using optical or microwave wavelengths, active or passive techniques, and diverse remote sensing data. However, the trade-off between the spatial and temporal resolutions of remote sensing imagery in detecting urban forests remains a challenge. For example, MODIS and Landsat series among satellite sensors may be the most commonly applied sensors because of their high revisit frequency capability and free availability [136].

The MODIS sensor obtains images of the same scene once a day but only captures ground resolution units in the range of 250–1000 m [137]. Although Landsat sensors can acquire images with a fine spatial resolution of 30 m, their revisit period is up to 16 days. In addition, the actual temporal resolution is much coarser owing to cloud contamination, which results in only a small number of Landsat images being available each year [138]. If high temporal frequency images cannot be fused with fine spatial resolution images in urban forest investigations, the available temporal–spatial resolution may not be satisfactorily obtained.

In the last few decades, quantification of forest biomass from LiDAR data has rapidly improved [11]. In forest structure and AGB estimation, tree height is an important structural feature. LiDAR is a suitable technique for measuring tree height and estimating forest AGB because of its ability to penetrate the forest canopy and record reflected signals from the top of the canopy and the ground [139]. LiDAR-derived metrics are usually based on digital elevation models (DEMs). An accurate DEM is critical for estimating tree height from LiDAR, as any errors contained in the DEM are propagated to the height estimation [140]. However, the resolution and efficiency issues may limit a wide application of the LiDAR-derived DEM method. Recently, LiDAR-derived DEMs have been greatly simplified by using statistical resampling methods. A DEM is obtained in a wide range of pixel sizes, and a series of statistical metrics are given for different pixels, proposing a method to calculate the minimum value. The LiDAR-derived DEM method shortens the time of processing and reduces error [141]. The method has great promise for future applications in tree height measurement and biomass estimation.

Cost-effectiveness may be a key issue in large-scale urban tree detection [142,143]. The cost of data procurement and processing limits the extent to which LiDAR can be used in large-scale research. Reducing the density of LiDAR points is a viable solution for forest assessment at a regional scale without compromising the accuracy of forest biomass estimation, and developing an appropriate point cloud density can be used to improve these estimates further [11]. High-resolution remote sensing imaging can be recommended as a cost-effective method for providing adequate local and temporal difference data.

In terms of applicability, different research methods involve different levels of forests and use data from different forest structures and types. For example, the 2D (e.g., optical passive remote sensing) methods usually use a sky perspective and technically can only distinguish tree canopies in the upper layer of the forest [128,144]. The 3D methods based on ALS have weaknesses when it comes to identifying understory trees and quantifying tree variables [145,146]. This is due to the reduced signal density of LiDAR data while penetrating the canopy [81]. In general, the TLS method can be used to retrieve more detailed information on tree inventory parameters [147]. However, the TLS method is only used to detect dense and vertical forest stems and cannot be used to separate individual trees [148]. This restriction may affect the visual quality of the images derived from LiDAR and the estimation of the tree variables. The combination of LiDAR and passive optical image data has been presented to improve the estimation of AGB and stand volume. Zhang and Shao [129] have combined LiDAR data with high-resolution images to quantitatively estimate forest biomass in Zhuhai city and improved the inversion accuracy. Thus, fusing LiDAR data and spectral data can provide a complete image of trees without blind spots, allowing visual assessment without viewpoint limitation.

4.3. Deep Learning in Tree Detection

In recent years, deep learning methods have been proposed for vegetation-related applications [149,150]. For example, deep learning-based object detection methods have been proven to help retrieve the locations of individual tree crowns. The dense convolutional network is one of the latest neural networks for visual object detection used to classify dominant tree species in highly complex urban environments [151]. Using deep learning techniques to identify trees at high risk of pest infestation can also enable decision makers to proactively prevent, monitor, and manage forest invasions of invasive species outbreaks with a high temporal resolution [152]. In particular, in the CNN architec-

tures, Mask R-CNN achieved excellent performance and outperformed other architectures designed for instance segmentation tasks [153], becoming the most promising publicly available framework for the core instance segmentation model for tree inventory generation workflow [154]. Yang et al. [155] used the Mask R-CNN model successfully to detect and locate individual tree crowns in New York's Central Park from Google Earth images.

The Mask R-CNN model has a powerful detection algorithm for fast and accurate identification with a strong model generalization ability for tree crown detection [156,157]. This method uses images from UAVs and Google Earth [158–160]. The accuracy of crown detection is affected by labels which exhibit different shape, size, texture, and chromaticity attributes. Therefore, t overlearn and overfitting must be avoided. In addition, in detecting isolated trees, this model can identify individual tree crowns in closed forests. However, identifying broadleaved tree canopies is more difficult because they are relatively flat, though closed conifers may be easily detected because they have conical crowns [154]. As a typical tool for machine learning, the Mask R-CNN model is an automatic extension to the naked eye and it may not be completely free from subjective constraints on labeling.

Overall, the proposed detection methods based on deep learning have some drawbacks. Tree detection based on high-resolution images remains underdeveloped. The object-based CNN method may produce a higher accuracy when manually generating training networks with samples for very high-resolution multispectral images [161]. However, it may not always be feasible to prepare training samples manually due to constraints of time and cost [162]. It is not easy to obtain ground truth information for constructing pixel-labeled datasets to train models. R-CNN bounding box detection (which becomes cuboid detection in 3D) is rigid and does not follow the contour of the tree crown, which is usually more circular [163]. Therefore, applying this method to crown detection can cause uncertainty.

4.4. Data Mining Approaches Using Street View Images

Oven the past few years, street-level mapping images from online products, such as Google Street Views, Baidu Maps, and Mapillary, have gradually become available to the public [164]. Street view images can better capture individual vegetation from a ground-based perspective [165] and implement virtual inventories of roadside trees to complement field data collection. These images can reduce labor, time, cost, and safety risks compared with field measurements [166]. Compared to other geospatial technologies, street view images are easy to operate and can be freely obtained. Regardless of the weather or seasonal conditions, virtual surveys based on street view images can be conducted throughout the year [167]. Street view images are expected to continue to be used as geospatial tools to assist in urban forestry research and practice [168]. Recently, research on autonomous vehicle technology has facilitated the development of methods based on large-scale street-level images [169]. For example, Xia et al. [170] have proposed an automatic image semantic segmentation method based on street view images to calculate the panoramic green view index to evaluate the greening condition of urban streets. However, street view imaging is biased towards the street, and, currently, it cannot yet fully cover parks and open areas. Until urban areas are fully covered, street view images can be supplemented by satellite or UAV imaging to cover missing areas.

5. Conclusions

Conventional field measurement methods can accurately capture information on forest features. Remote sensing provides an alternative method for biomass measurements at different temporal and spatial resolutions. Currently, the trend in urban forest detection is to integrate multiple methods with increased temporal and spatial resolution to monitor urban forests. Fusing LiDAR and spectral data is very helpful in improving detection accuracy. However, urban forest surveys based on remote sensing data remain a critical and challenging task. Continuous acquisition of UAV measurements and field observations is essential for estimating and calibrating satellite-derived urban forest data. The Mask

R-CNN model can obtain detailed information about tree crowns based on UAV and remote sensing images as an automatic extension of the naked eye. Recent advances in object detection techniques in deep learning have provided a method for automatically detecting urban forest features captured in street view images. An integrated framework that includes multiple scales, disciplines, and locations is a possible way to quantify and better understand urban forests at different spatiotemporal scales. This review describes the applications of low-cost, high-spatial resolution, multidimensional, and big data methods in urban forests. Integrating field observations and remote sensing data with urban forest models and deep learning methods provides a promising direction. These methods will improve our understanding of the characteristics of urban forests and significantly enhance their management.

Author Contributions: M.Y. and C.P. conceived the study; M.Y. and X.Z. led and carried out all of the analyses; Z.L., P.L., J.T. and B.X. collected and analyzed the data; M.Y. and X.Z. led the writing of the manuscript. All authors contributed critically to the drafts and gave final approval for publication. All authors have read and agreed to the published version of the manuscript.

Funding: This study was supported financially by the Key Research and Development Program of Hunan Province (2021NK2031), the outstanding Youth Project of the Hunan Provincial Education Department (19B350), the National Natural Science Foundation of China (41901117), Natural Science Foundation of Hunan Province, China (2020JJ5362), and the Natural Sciences and Engineering Research Council of Canada (NSERC) Discovery Grant.

Institutional Review Board Statement: Not applicable.

Informed Consent Statement: Not applicable.

Data Availability Statement: Not applicable.

Conflicts of Interest: The authors declare no conflict of interest.

References

1. Byomkesh, T.; Nakagoshi, N.; Dewan, A.M. Urbanization and green space dynamics in Greater Dhaka, Bangladesh. *Landsc. Ecol. Eng.* **2012**, *8*, 45–58. [CrossRef]
2. Ives, C.D.; Lentini, P.E.; Threlfall, C.G.; Ikin, K.; Shanahan, D.F.; Garrard, G.E.; Bekessy, S.A.; Fuller, R.A.; Mumaw, L.; Rayner, L.; et al. Cities are hotspots for threatened species. *Glob. Ecol. Biogeogr.* **2016**, *25*, 117–126. [CrossRef]
3. Zhao, S.; Da, L.; Tang, Z.; Fang, H.; Song, K.; Fang, J. Ecological consequences of rapid urban expansion: Shanghai, China. *Environ. Front. Ecol. Environ.* **2006**, *4*, 341–346. [CrossRef]
4. Lin, B.; Zhu, J. Changes in urban air quality during urbanization in China. *J. Clean. Prod.* **2018**, *188*, 312–321. [CrossRef]
5. Zhou, X.; Wang, Y. Spatial–temporal dynamics of urban green space in response to rapid urbanization and greening policies. *Landsc. Urban Plan.* **2011**, *100*, 268–277. [CrossRef]
6. Zhao, S.; Liu, S.; Zhou, D. Prevalent vegetation growth enhancement in urban environment. *Proc. Natl. Acad. Sci. USA* **2016**, *113*, 6313–6318. [CrossRef]
7. Davies, Z.G.; Dallimer, M.; Edmondson, J.L.; Leake, J.R.; Gaston, K.J. Identifying potential sources of variability between vegetation carbon storage estimates for urban areas. *Environ. Pollut.* **2013**, *183*, 133–142. [CrossRef]
8. Nowak, D.J.; Greenfield, E.J.; Hoehn, R.E.; Lapoint, E. Carbon storage and sequestration by trees in urban and community areas of the United States. *Environ. Pollut.* **2013**, *178*, 229–236. [CrossRef]
9. Lin, J.; Kroll, C.N.; Nowak, D.J.; Greenfield, E.J. A review of urban forest modeling: Implications for management and future research. *Urban For. Urban Green* **2019**, *43*, 126366. [CrossRef]
10. Sinha, S.; Jeganathan, C.; Sharma, L.K.; Nathawat, M.S. A review of radar remote sensing for biomass estimation. *Environ. Sci. Technol. Int. J. Environ. Sci. Technol.* **2015**, *12*, 1779–1792. [CrossRef]
11. Singh, K.K.; Chen, G.; McCarter, J.B.; Meentemeyer, R.K. Effects of LiDAR point density and landscape context on estimates of urban forest biomass. *ISPRS J. Photogramm. Remote Sens.* **2015**, *101*, 310–322. [CrossRef]
12. McHale, M.R.; Burke, I.C.; Lefsky, M.A.; Peper, P.J.; McPherson, E.G. Urban forest biomass estimates: Is it important to use allometric relationships developed specifically for urban trees? *Urban Ecosyst.* **2009**, *12*, 95–113. [CrossRef]
13. Duncanson, L.I.; Cook, B.D.; Hurtt, G.C.; Dubayah, R.O. An efficient, multi-layered crown delineation algorithm for mapping individual tree structure across multiple ecosystems. *Remote Sens. Environ.* **2014**, *154*, 378–386. [CrossRef]
14. Zhang, C.; Zhou, Y.; Qiu, F. Individual tree segmentation from LiDAR point clouds for urban forest inventory. *Remote Sens.* **2015**, *7*, 7892–7913. [CrossRef]

15. Nowak, D.J.; Dwyer, J.F. Understanding the benefits and costs of urban forest ecosystems. In *Urban and Community Forestry in the Northeast*; Springer: Dordrecht, The Netherlands, 2007; pp. 25–46.
16. Jutras, P.; Prasher, S.O.; Mehuys, G.R. Prediction of street tree morphological parameters using artificial neural networks. *Comput. Electron. Agric.* **2009**, *67*, 9–17. [CrossRef]
17. Jaakkola, A.; Hyyppä, J.; Kukko, A.; Yu, X.; Kaartinen, H.; Lehtomäki, M.; Lin, Y. A low-cost multi-sensoral mobile mapping system and its feasibility for tree measurements. *ISPRS J. Photogramm. Remote Sens.* **2010**, *65*, 514–522. [CrossRef]
18. Raumonen, P.; Kaasalainen, M.; Markku, Å.; Kaasalainen, S.; Kaartinen, H.; Vastaranta, M.; Holopainen, M.; Disney, M.; Lewis, P. Fast automatic precision tree models from terrestrial laser scanner data. *Remote Sens.* **2013**, *5*, 491–520. [CrossRef]
19. Song, C. Optical remote sensing of forest leaf area index and biomass. *Prog. Phys. Geogr.* **2013**, *37*, 98–113. [CrossRef]
20. Zeng, L.; Lu, J.; Li, W.; Li, Y. A fast approach for large-scale Sky View Factor estimation using street view images. *Build. Environ.* **2018**, *135*, 74–84. [CrossRef]
21. Puliti, S.; Saarela, S.; Gobakken, T.; Ståhl, G.; Næsset, E. Combining UAV and Sentinel-2 auxiliary data for forest growing stock volume estimation through hierarchical model-based inference. *Remote Sens. Environ.* **2018**, *204*, 485–497. [CrossRef]
22. Xi, Z.; Hopkinson, C.; Rood, S.B.; Peddle, D.R. See the forest and the trees: Effective machine and deep learning algorithms for wood filtering and tree species classification from terrestrial laser scanning. *ISPRS J. Photogramm. Remote Sens.* **2020**, *168*, 1–16. [CrossRef]
23. Zhao, S.; Zhu, C.; Zhou, D.; Huang, D.; Werner, J. Organic carbon storage in China's urban areas. *PLoS ONE* **2013**, *8*, e71975. [CrossRef] [PubMed]
24. Boukili, V.K.S.; Bebber, D.P.; Mortimer, T.; Venicx, G.; Lefcourt, D.; Chandler, M.; Eisenberg, C. Assessing the performance of urban forest carbon sequestration models using direct measurements of tree growth. Urban For. *Urban Green* **2017**, *24*, 212–221. [CrossRef]
25. Malhi, Y.; Phillips, O.L.; Lloyd, J.; Baker, T.; Wright, J.; Almeida, S.; Arroyo, L. An international network to monitor the structure, composition and dynamics of Amazonian forests (RAINFOR). *Appl. Veg. Sci.* **2002**, *13*, 439–450. [CrossRef]
26. Timilsina, N.; Staudhammer, C.L.; Escobedo, F.J.; Lawrence, A. Tree biomass, wood waste yield, and carbon storage changes in an urban forest. *Landsc. Urban Plan.* **2014**, *127*, 18–27. [CrossRef]
27. Návar, J. Allometric equations for tree species and carbon stocks for forests of northwestern Mexico. *For. Ecol. Manag.* **2009**, *257*, 427–434. [CrossRef]
28. Zhao, S.Q.; Liu, S.; Li, Z.; Sohl, T.L. A spatial resolution threshold of land cover in estimating terrestrial carbon sequestration in four counties in Georgia and Alabama, USA. *Biogeosciences* **2010**, *7*, 71–80. [CrossRef]
29. Jo, H.K.; McPherson, E.G. Indirect carbon reduction by residential vegetation and planting strategies in Chicago, USA. *J. Environ. Manag.* **2001**, *61*, 165–177. [CrossRef]
30. McPherson, E.G.; van Doorn, N.; Peper, P.J. Urban Tree Database and Allometric Equations. In *General Technical Report PSW-GTR-253*; US Department of Agriculture, Forest Service, Pacific Southwest Research Station: Albany, CA, USA, 2016; p. 86.
31. Yoon, T.K.; Park, C.W.; Lee, S.J.; Ko, S.; Kim, K.N.; Son, Y.; Lee, K.H.; Oh, S.; Lee, W.K.; Son, Y. Allometric equations for estimating the aboveground volume of five common urban street tree species in Daegu, Korea. Urban For. *Urban Green* **2013**, *12*, 344–349. [CrossRef]
32. Pillsbury, N.H.; Reimer, J.L.; Thompson, R.P. Tree volume equations for 10 urban species in California. In *Technical Coordinators, Proceedings of a Symposium on Oak Woodlands: Ecology, Management, and Urban Interface Issues, San Luis Obispo, CA, USA, 19–22 March 1996*; Urban Forest Ecosystems Institute, California Polytechnic State University: Albany, CA, USA, 1997.
33. Tanhuanpää, T.; Kankare, V.; Setälä, H.; Yli-Pelkonen, V.; Vastaranta, M.; Niemi, M.T.; Raisio, J.; Holopainen, M. Assessing above-ground biomass of open-grown urban trees: A comparison between existing models and a volume-based approach. *Urban For. Urban Green* **2017**, *21*, 239–246. [CrossRef]
34. Nowak, D.J.; Crane, D.E. Carbon storage and sequestration by urban trees in the USA. *Environ. Pollut.* **2002**, *116*, 381–389. [CrossRef]
35. Ketterings, Q.M.; Coe, R.; Van Noordwijk, M.; Ambagau, Y.; Palm, C.A. Reducing uncertainty in the use of allometric biomass equations for predicting above-ground tree biomass in mixed secondary forests. *For. Ecol. Manag.* **2001**, *146*, 199–209. [CrossRef]
36. Nowak, D.J. Atmospheric carbon dioxide reduction by Chicago's urban forest. In *Chicago's Urban Forest Ecosystem: Results of the Chicago Urban Forest Climate Project*; U.S. Department of Agriculture, Forest Service, Northeastern Forest Experiment Station: Washington, DC, USA, 1994; pp. 83–94.
37. Aguaron, E.; McPherson, E.G. Comparison of methods for estimating carbon dioxide storage by Sacramento's urban forest. In *Carbon Sequestration in Urban Ecosystems*; Springer: Dordrecht, The Netherlands, 2012; pp. 43–71.
38. Sileshi, G.W. A critical review of forest biomass estimation models, common mistakes and mistakes and corrective measures. *For. Ecol. Manag.* **2014**, *329*, 237–254. [CrossRef]
39. Picard, N.; Boyemba Bosela, F.; Rossi, V. Reducing the error in biomass estimates strongly depends on model selection. *Ann. For. Sci.* **2015**, *72*, 811–823. [CrossRef]
40. Van Breugel, M.; Ransijn, J.; Craven, D.; Bongers, F.; Hall, J.S. Estimating carbon stock in secondary forests: Decisions and uncertainties associated with allometric biomass models. *For. Ecol. Manag.* **2011**, *262*, 1648–1657. [CrossRef]
41. Wu, J. Developing general equations for urban tree biomass estimation with high-resolution satellite imagery. *Sustainability* **2019**, *11*, 4347. [CrossRef]

42. Mohd Zaki, N.A.; Abd Latif, Z. Carbon sinks and tropical forest biomass estimation: A review on role of remote sensing in aboveground-biomass modelling. *Geocarto Int.* **2017**, *32*, 701–716. [CrossRef]
43. Huang, Y.; Yu, B.; Zhou, J.; Hu, C.; Tan, W.; Hu, Z.; Wu, J. Toward automatic estimation of urban green volume using airborne LiDAR data and high resolution Remote Sensing images. *Front. Earth Sci.* **2013**, *7*, 43–54. [CrossRef]
44. Pu, R.; Landry, S. A comparative analysis of high spatial resolution IKONOS and WorldView-2 imagery for mapping urban tree species. *Remote Sens. Environ.* **2012**, *124*, 516–533. [CrossRef]
45. Galidaki, G.; Zianis, D.; Gitas, I.; Radoglou, K.; Karathanassi, V.; Tsakiri-Strati, M.; Woodhouse, I.; Mallinis, G. Vegetation biomass estimation with remote sensing: Focus on forest and other wooded land over the Mediterranean ecosystem. *Int. J. Remote Sens.* **2017**, *38*, 1940–1966. [CrossRef]
46. Ji, L.; Wylie, B.K.; Nossov, D.R.; Peterson, B.; Waldrop, M.P.; McFarland, J.W.; Rover, J.; Hollingsworth, T.N. Estimating aboveground biomass in interior Alaska with Landsat data and field measurements. *Int. J. Appl. Earth Obs. Geoinf.* **2012**, *18*, 451–461. [CrossRef]
47. Shen, G.; Wang, Z.; Liu, C.; Han, Y. Mapping aboveground biomass and carbon in Shanghai's urban forest using Landsat ETM+ and inventory data. *Urban For. Urban Green.* **2020**, *51*, 126655. [CrossRef]
48. Deo, R.K.; Russell, M.B.; Domke, G.M.; Andersen, H.E.; Cohen, W.B.; Woodall, C.W. Evaluating site-specific and generic spatial models of aboveground forest biomass based on landsat Time-Series and LiDAR strip samples in the Eastern USA. *Remote Sens.* **2017**, *9*, 598. [CrossRef]
49. Zhao, S.; Zhou, D.; Zhu, C.; Sun, Y.; Wu, W.; Liu, S. Spatial and temporal dimensions of urban expansion in China. *Environ. Sci. Technol.* **2015**, *49*, 9600–9609. [CrossRef] [PubMed]
50. Uniyal, S.; Purohit, S.; Chaurasia, K.; Rao, S.S.; Amminedu, E. Quantification of carbon sequestration by urban forest using Landsat 8 OLI and machine learning algorithms in Jodhpur, India. *Urban For. Urban Green* **2022**, *67*, 127445. [CrossRef]
51. Myeong, S.; Nowak, D.J.; Duggin, M.J. A temporal analysis of urban forest carbon storage using remote sensing. *Remote Sens. Environ.* **2006**, *101*, 277–282. [CrossRef]
52. González-Jaramillo, V.; Fries, A.; Zeilinger, J.; Homeier, J.; Paladines-Benitez, J.; Bendix, J. Estimation of above ground biomass in a tropical mountain forest in southern Ecuador using airborne LiDAR data. *Remote Sens.* **2018**, *10*, 660. [CrossRef]
53. Paul, K.I.; Roxburgh, S.H.; Chave, J.; England, J.R.; Zerihun, A.; Specht, A.; Lewis, T.; Bennett, L.T. Testing the generality of above-ground biomass allometry across plant functional types at the continent scale. *Glob. Chang. Biol.* **2016**, *22*, 2106–2124. [CrossRef]
54. Palace, M.; Keller, M.; Asner, G.P.; Hagen, S.; Braswell, B. Amazon forest structure from IKONOS satellite data and the automated characterization of forest canopy properties. *Biotropica.* **2008**, *40*, 141–150. [CrossRef]
55. Wolter, P.T.; Townsend, P.A.; Sturtevant, B.R. Estimation of forest structural parameters using 5 and 10 meter SPOT-5 satellite data. *Remote Sens. Environ.* **2009**, *113*, 2019–2036. [CrossRef]
56. Nichol, J.; Wong, M.S. Remote sensing of urban vegetation life form by spectral mixture analysis of high-resolution IKONOS satellite images. *Int. J. Remote Sens.* **2007**, *28*, 985–1000. [CrossRef]
57. Tooke, T.R.; Coops, N.C.; Goodwin, N.R.; Voogt, J.A. Extracting urban vegetation characteristics using spectral mixture analysis and decision tree classifications. *Remote Sens. Environ.* **2009**, *113*, 398–407. [CrossRef]
58. Mcpherson, E.G.; Xiao, Q.; Aguaron, E. A new approach to quantify and map carbon stored, sequestered and emissions avoided by urban forests. *Landsc. Urban Plan.* **2013**, *120*, 70–84. [CrossRef]
59. Bendix, J.; Rollenbeck, R.; Palacios, E. Cloud detection in the tropics—A suitable tool for climate-ecological studies in the high mountains of Ecuador. *Int. J. Remote Sens.* **2004**, *25*, 4521–4540. [CrossRef]
60. Magnussen, S.; Nord-Larsen, T.; Riis-Nielsen, T. Lidar supported estimators of wood volume and aboveground biomass from the Danish national forest inventory (2012–2016). *Remote Sens. Environ.* **2018**, *211*, 146–153. [CrossRef]
61. Goldbergs, G.; Levick, S.R.; Lawes, M.; Edwards, A. Hierarchical integration of individual tree and area-based approaches for savanna biomass uncertainty estimation from airborne LiDAR. *Remote Sens. Environ.* **2018**, *205*, 141–150. [CrossRef]
62. Piiroinen, R.; Heiskanen, J.; Maeda, E.; Viinikka, A.; Pellikka, P. Classification of tree species in a diverse African Agroforestry landscape using imaging spectroscopy and laser scanning. *Remote Sens.* **2017**, *9*, 875. [CrossRef]
63. Posilero, M.A.V.; Paringit, E.C.; Argamosa, R.J.L.; Faelga, R.A.G.; Ibanez, C.A.G.; Zaragosa, G.P. Lidar-Based canopy cover estimation using linear regression techniques. *J. Philipp. Geosci. Remote Sens. Soc.* **2016**, *2*, 26–33.
64. Speak, A.; Escobedo, F.J.; Russo, A.; Zerbe, S. Total urban tree carbon storage and waste management emissions estimated using a combination of LiDAR, field measurements and an end-of-life wood approach. *J. Clean. Prod.* **2020**, *256*, 120420. [CrossRef]
65. Alonzo, M.; Bookhagen, B.; Roberts, D.A. Urban trees species mapping using hyperspectral and lidar data fusion. *Remote Sens. Environ.* **2014**, *148*, 70–83. [CrossRef]
66. Laurin, G.V.; Chen, Q.; Lindsell, J.A.; Coonmes, D.A.; Del Frate, F.; Guerriero, L. Above ground biomass estimation in an African tropical forest with lidar and hyperspectral data. *ISPRS J. Photogramm. Remote Sens.* **2014**, *89*, 49–58. [CrossRef]
67. Srinivasan, S.; Popescu, S.C.; Eriksson, M.; Sheridan, R.D.; Ku, N.W. Multi-temporal terrestrial laser scanning for modeling tree biomass change. *For. Ecol. Manag.* **2014**, *318*, 304–317. [CrossRef]
68. Gonzalez, P.; Asner, G.P.; Battles, J.J.; Lefsky, M.A.; Waring, K.M.; Palace, M. Forest carbon densities and uncertainties from Lidar, QuickBird, and field measurements in California. *Remote Sens. Environ.* **2010**, *114*, 1561–1575. [CrossRef]

69. Edson, C.; Wing, M.G. Airborne light detection and ranging (LiDAR) for individual tree stem location, height, and biomass measurements. *Remote Sens.* **2011**, *3*, 2494–2528. [CrossRef]
70. Othmani, A.; Lew Yan Voon, L.F.C.; Stolz, C.; Piboule, A. Single tree species classification from Terrestrial Laser Scanning data for forest inventory. *Pattern Recognit. Lett.* **2013**, *34*, 2144–2150. [CrossRef]
71. Wu, B.; Yu, B.; Yue, W.; Shu, S.; Tan, W.; Hu, C.; Huang, Y.; Wu, J.; Liu, H. A voxel-based method for automated identification and morphological parameters estimation of individual street trees from mobile laser scanning data. *Remote Sens.* **2013**, *5*, 584–611. [CrossRef]
72. Koch, B.; Heyder, U.; Weinacker, H. Detection of individual tree crowns in airborne lidar data. *Photogramm. Eng. Remote Sens.* **2006**, *72*, 357–363. [CrossRef]
73. Næsset, E. Airborne laser scanning as a method in operational forest inventory: Status of accuracy assessments accomplished in Scandinavia. *Scand. J. For. Res.* **2007**, *22*, 433–442. [CrossRef]
74. Matasci, G.; Coops, N.C.; Williams, D.A.R.; Page, N. Mapping tree canopies in urban environments using airborne laser scanning (ALS): A Vancouver case study. *For. Ecosyst.* **2018**, *5*, 31. [CrossRef]
75. Zhang, C.; Qiu, F. Mapping individual tree species in an urban forest using airborne lidar data and hyperspectral imagery. *Photogramm. Eng. Remote Sens.* **2012**, *78*, 1079–1087. [CrossRef]
76. Liu, L.; Coops, N.C.; Aven, N.W.; Pang, Y. Mapping urban tree species using integrated airborne hyperspectral and LiDAR remote sensing data. *Remote Sens. Environ.* **2017**, *200*, 170–182. [CrossRef]
77. Lim, K.; Treitz, P.; Wulder, M.; St-Ongé, B.; Flood, M. LiDAR remote sensing of forest structure. *Prog. Phys. Geogr.* **2003**, *27*, 88–106. [CrossRef]
78. Kankare, V.; Liang, X.; Vastaranta, M.; Yu, X.; Holopainen, M.; Hyyppä, J. Diameter distribution estimation with laser scanning based multisource single tree inventory. *ISPRS J. Photogramm. Remote Sens.* **2015**, *108*, 161–171. [CrossRef]
79. Dassot, M.; Constant, T.; Fournier, M. The use of terrestrial LiDAR technology in forest science: Application fields, benefits and challenges. *Ann. For. Sci.* **2011**, *68*, 959–974. [CrossRef]
80. Lindberg, E.; Holmgren, J.; Olofsson, K. Estimation of stem attributes using a combination of terrestrial and airborne laser scanning. *Eur. J. For. Res.* **2012**, *131*, 1917–1931. [CrossRef]
81. Hu, S.; Li, Z.; Zhang, Z.; He, D.; Wimmer, M. Efficient tree modeling from airborne LiDAR point clouds. *Comput. Gr.* **2017**, *67*, 1–13. [CrossRef]
82. Fernández-Sarría, A.; Velázquez-Martí, B.; Sajdak, M.; Martínez, L.; Estornell, J. Residual biomass calculation from individual tree architecture using terrestrial laser scanner and ground-level measurements. *Comput. Electron. Agric.* **2013**, *93*, 90–97. [CrossRef]
83. Lehtomä, M.; Jaakkola, A.; Hyyppä, J. Detection of vertical pole-like objects in a road environment using vehicle-based laser scanning data. *Remote Sens.* **2010**, *2*, 641–664. [CrossRef]
84. Yang, B.; Wei, Z.; Li, Q.; Li, J. Automated extraction of street-scene objects from mobile lidar point clouds. *Int. J. Remote Sens.* **2014**, *33*, 5839–5861. [CrossRef]
85. Guan, H.; Yu, Y.; Ji, Z.; Li, J.; Zhang, Q. Deep learning-based tree classification using mobile LiDAR data. *Remote Sens Lett.* **2015**, *6*, 864–873. [CrossRef]
86. Erdody, T.L.; Moskal, L.M. Fusion of LiDAR and imagery for estimating forest canopy fuels. *Remote Sens. Environ.* **2010**, *114*, 725–737. [CrossRef]
87. Næsset, E.; Økland, T. Estimating tree height and tree crown properties using airborne scanning laser in a boreal nature reserve. *Remote Sens. Environ.* **2002**, *79*, 105–115. [CrossRef]
88. Popescu, S.C.; Zhao, K. A voxel-based lidar method for estimating crown base height for deciduous and pine trees. *Remote Sens. Environ.* **2008**, *112*, 767–781. [CrossRef]
89. Chenari, A.; Erfanifard, Y.; Dehghani, M.; Pourghasemi, H.R. Woodland mapping at single-tree levels using object-oriented classification of unmanned aerial vehicle (UAV) images. *Int. Arch. Photogramm. Remote Sens. Spatial Inf. Sci.* **2017**, *42*, 43–49. [CrossRef]
90. Rango, A.; Laliberte, A.; Herrick, J.E.; Winters, C.; Havstad, K.; Steele, C.; Browning, D. Unmanned aerial vehicle-based remote sensing for rangeland assessment, monitoring, and management. *J. Appl. Remote Sens.* **2009**, *3*, 033542. [CrossRef]
91. Brieger, F.; Herzschuh, U.; Pestryakova, L.A.; Bookhagen, B.; Zakharov, E.S.; Kruse, S. Advances in the derivation of Northeast Siberian forest metrics using high-resolution UAV-based photogrammetric point clouds. *Remote Sens.* **2019**, *11*, 1447. [CrossRef]
92. Feng, Q.; Liu, J.; Gong, J. UAV remote sensing for urban vegetation mapping using random forest and texture analysis. *Remote Sens.* **2015**, *7*, 1074–1094. [CrossRef]
93. Onishi, M.; Ise, T. Automatic classification of trees using a UAV onboard camera and deep learning. *arXiv* **2018**, arXiv:1804.10390.
94. Feng, X.; Li, P. A tree species mapping method from UAV images over urban area using similarity in tree-crown object histograms. *Remote Sens.* **2019**, *11*, 1982. [CrossRef]
95. Mu, Y.; Fujii, Y.; Takata, D.; Zheng, B.; Noshita, K.; Honda, K.; Ninomiya, S.; Guo, W. Characterization of peach tree crown by using high-resolution images from an unmanned aerial vehicle. *Hortic. Res.* **2018**, *5*, 1–10. [CrossRef]
96. Yang, B.; Dai, W.; Dong, Z.; Liu, Y. Automatic forest mapping at individual tree levels from terrestrial laser scanning point clouds with a hierarchical minimum cut method. *Remote Sens.* **2016**, *8*, 372. [CrossRef]
97. Budei, B.C.; St-Onge, B.; Hopkinson, C.; Audet, F.A. Identifying the genus or species of individual trees using a three-wavelength airborne lidar system. *Remote Sens. Environ.* **2018**, *204*, 632–647. [CrossRef]

98. Wu, J.; Yao, W.; Polewski, P. Mapping individual tree species and vitality along urban road corridors with LiDAR and imaging sensors: Point density versus view perspective. *Remote Sens.* **2018**, *10*, 1403. [CrossRef]
99. Cowett, F.D. Methodology for spatial analysis of municipal street tree benefits. *Arboric Urban For.* **2014**, *40*, 112–118. [CrossRef]
100. McPherson, E.G. Selecting reference cities for i-Tree streets. *Arboric Urban For.* **2010**, *36*, 230–240. [CrossRef]
101. Peng, L.; Chen, S.; Liu, Y.; Wang, J. Application of CITYgreen model in benefit assessment of Nanjing urban green space in carbon fixation and runoff reduction. *Front. For. China* **2008**, *3*, 177–182. [CrossRef]
102. Lin, J.; Kroll, C.N.; Nowak, D.J. An uncertainty framework for i-Tree eco: A comparative study of 15 cities across the United States. *Urban For. Urban Green.* **2021**, *60*, 127062. [CrossRef]
103. Michael, Y.; Lensky, I.M.; Brenner, S.; Tchetchik, A.; Tessler, N.; Helman, D. Economic assessment of fire damage to urban forest in the wildland-urban interface using planet satellites constellation images. *Remote Sens.* **2018**, *10*, 1479. [CrossRef]
104. Nowak, D.J.; Crane, D.E.; Stevens, J.C.; Hoehn, R.E.; Walton, J.T.; Bond, J. A ground-based method of assessing urban forest structure and ecosystem services. *Arboric Urban For.* **2008**, *34*, 347–358. [CrossRef]
105. Lal, R.; Augustin, B. *Carbon Sequestration in Urban Ecosystems*; Springer Science & Business Media: Berlin, Germany, 2011. [CrossRef]
106. Zhu, X.X.; Tuia, D.; Mou, L.; Xia, G.S.; Zhang, L.; Xu, F.; Fraundorfer, F. Deep learning in remote sensing: A comprehensive review and list of resource. *IEEE Geosci. Remote Sens. Mag.* **2017**, *5*, 8–36. [CrossRef]
107. Minetto, R.; Pamplona Segundo, M.; Sarkar, S. Hydra: An ensemble of convolutional neural networks for geospatial land classification. *IEEE Trans. Geosci. Remote Sens.* **2019**, *57*, 6530–6541. [CrossRef]
108. Pleşoianu, A.I.; Stupariu, M.S.; Şandric, I.; Pătru-Stupariu, I.; Drăguţ, L. Individual tree-crown detection and species classification in very high-resolution remote sensing imagery using a deep learning ensemble model. *Remote Sens.* **2020**, *12*, 2426. [CrossRef]
109. Brandt, M.; Tucker, C.J.; Kariryaa, A.; Rasmussen, K.; Abel, C.; Small, J.; Chave, J.; Rasmussen, L.V.; Hiernaux, P.; Diouf, A.A.; et al. An unexpectedly large count of trees in the West African Sahara and Sahel. *Nature* **2020**, *587*, 78–82. [CrossRef] [PubMed]
110. Weinstein, B.G.; Marconi, S.; Bohlman, S.; Zare, A.; White, E. Individual tree-crown detection in RGB imagery using semi-supervised deep learning neural networks. *Remote Sens.* **2019**, *11*, 1309. [CrossRef]
111. Li, Y.; Li, M.; Li, C.; Liu, Z. Forest aboveground biomass estimation using Landsat 8 and Sentinel-1A data with machine learning algorithms. *Sci. Rep.* **2020**, *10*, 1–12. [CrossRef]
112. Wegner, J.D.; Branson, S.; Hall, D.; Schindler, K.; Perona, P. Cataloging public objects using aerial and street-level images-urban trees. In Proceedings of the 2016 IEEE Conference on Computer Vision and Pattern Recognition (CVPR), Las Vegas, NV, USA, 27–30 June 2016; pp. 6014–6023. [CrossRef]
113. Li, W.; Fu, H.; Yu, L.; Cracknell, A. Deep learning based oil palm tree detection and counting for high-resolution remote sensing images. *Remote Sens.* **2017**, *9*, 22. [CrossRef]
114. Hackel, T.; Savinov, N.; Ladicky, L.; Wegner, J.D.; Schindler, K.; Pollefeys, M. Semantic3d net: A new large-scale point cloud classification benchmark. *arXiv* **2017**, arXiv:1704.03847.
115. Khamparia, A.; Singh, K.M. A systematic review on deep learning architectures and applications. *Expert Syst.* **2019**, *36*, 1–22. [CrossRef]
116. Li, X.; Ratti, C.; Seiferling, I. Quantifying the shade provision of street trees in urban landscape: A case study in Boston, USA, using Google Street View. *Landsc. Urban Plan.* **2018**, *169*, 81–91. [CrossRef]
117. Berland, A.; Lange, D.A. Google street view shows promise for virtual street tree surveys. *Urban For. Urban Green* **2017**, *21*, 11–15. [CrossRef]
118. Li, X.; Ratti, C. Mapping the spatial distribution of shade provision of street trees in Boston using Google Street View panoramas. *Urban For. Urban Green* **2018**, *31*, 109–119. [CrossRef]
119. Zhou, X.; Kim, J. Social disparities in tree canopy and park accessibility A case study of six cities in Illinois using GIS and remote sensing. *Urban For. Urban Green.* **2013**, *12*, 88–97. [CrossRef]
120. Stubbings, P.; Peskett, J.; Rowe, F.; Arribas-Bel, D. A hierarchical Urban forest index using street-level imagery and deep learning. *Remote Sens.* **2019**, *11*, 1395. [CrossRef]
121. Li, X.; Fellow, P.; Studies, U.; Room, T.; Avenue, M.; Yang, B.; Studies, U.; Ratti, T.C.; Studies, U. Using street-level images and deep learning for urban landscape studies. *Landsc. Archit. Front.* **2018**, *6*, 20–29. [CrossRef]
122. Zhang, Y.; Middel, A.; Turner, B.L. Evaluating the effect of 3D urban form on neighborhood land surface temperature using Google Street View and geographically weighted regression. *Landsc. Ecol.* **2019**, *34*, 681–697. [CrossRef]
123. Lu, D. Aboveground biomass estimation using Landsat TM data in the Brazilian Amazon. *Int. J. Remote Sens.* **2005**, *26*, 2509–2525. [CrossRef]
124. Pandit, S.; Tsuyuki, S.; Dube, T. Landscape-scale aboveground biomass estimation in buffer zone community forests of Central Nepal: Coupling in situ measurements with Landsat 8 Satellite Data. *Remote Sens.* **2018**, *10*, 1848. [CrossRef]
125. Clark, D.B.; Clark, D.A. Landscape-scale variation in forest structure and biomass in a tropical rain forest. *For. Ecol. Manag.* **2000**, *137*, 185–198. [CrossRef]
126. Saatchi, S.S.; Harris, N.L.; Brown, S.; Lefsky, M.; Mitchard, E.T.A.; Salas, W.; Zutta, B.R. Benchmark map of forest carbon stocks in tropical regions across three continents. *Proc. Natl. Acad. Sci. USA* **2011**, *108*, 9899–9904. [CrossRef]

127. Powell, S.L.; Cohen, W.B.; Healey, S.P.; Kennedy, R.E.; Moisen, G.G.; Pierce, K.B.; Ohmann, J.L. Quantification of live aboveground forest biomass dynamics with Landsat time-series and fi eld inventory data: A comparison of empirical modeling approaches. *Remote Sens. Environ.* **2010**, *114*, 1053–1068. [CrossRef]
128. Heinzel, J.N.; Weinacker, H.; Koch, B. Prior-knowledge-based single-tree extraction. *Int. J. Remote Sens.* **2011**, *32*, 4999–5020. [CrossRef]
129. Xia, S.; Wang, C.; Pan, F.; Xi, X.; Zeng, H.; Liu, H. Detecting stems in dense and homogeneous forest using single-scan TLS. *Forests* **2015**, *6*, 3923–3945. [CrossRef]
130. Patenaude, G.; Milne, R.; Dawson, T.P. Synthesis of remote sensing approaches for forest carbon estimation: Reporting to the Kyoto Protocol. *Environ. Sci. Policy* **2005**, *8*, 161–178. [CrossRef]
131. Kumar, L.; Onisimo, M. Remote sensing of above-ground biomass. *Remote Sens.* **2017**, *9*, 935. [CrossRef]
132. Ganivet, E.; Bloomberg, M. Towards rapid assessments of tree species diversity and structure in fragmented tropical forests: A review of perspectives offered by remotely-sensed and field-based data. *For. Ecol. Manag.* **2019**, *432*, 40–53. [CrossRef]
133. Sant, E.D.; Simonds, G.E.; Ramsey, R.D.; Larsen, R.T. Assessment of sagebrush cover using remote sensing at multiple spatial and temporal scales. *Ecol. Indic.* **2014**, *43*, 297–305. [CrossRef]
134. da Cunha Neto, E.M.; Rex, F.E.; Veras, H.F.P.; Moura, M.M.; Sanquetta, C.R.; Käfer, P.S.; Sanquetta, M.N.I.; Zambrano, A.M.A.; Broadbent, E.N.; Dalla Corte, A.P. Using high-density UAV-Lidar for deriving tree height of Araucaria Angustifolia in an Urban Atlantic Rain Forest. *Urban For. Urban Green.* **2021**, *63*, 127197. [CrossRef]
135. Yang, X.; Liu, Y.; Wu, Z.; Yu, Y.; Li, F.; Fan, W. Forest age mapping based on multiple-resource remote sensing data. *Environ. Monit. Assess.* **2020**, *192*, 1–15. [CrossRef]
136. Agrawal, S.; Khairnar, G.B. A comparative assessment of remote sensing imaging techniques: Optical, SAR and LiDAR. *Int. Arch. Photogramm. Remote Sens.* **2019**, *XLII-5/W3*, 1–6. [CrossRef]
137. Wang, Q.; Tang, Y.; Tong, X.; Atkinson, P.M. Virtual image pair-based spatio-temporal fusion. *Remote Sens. Environ.* **2020**, *249*, 112009. [CrossRef]
138. Roy, D.P.; Wulder, M.A.; Loveland, T.R.; Woodcock, C.E.; Allen, R.G.; Anderson, M.C.; Helder, D.; Irons, J.R.; Johnson, D.M.; Kennedy, R.; et al. Landsat-8: Science and product vision for terrestrial global change research. *Remote Sens. Environ.* **2014**, *145*, 154–172. [CrossRef]
139. Lin, J.; Chen, D.; Wu, W.; Liao, X. Estimating aboveground biomass of urban forest trees with dual-source UAV acquired point clouds. *Urban For. Urban Green.* **2022**, *69*, 127521. [CrossRef]
140. Tinkham, W.T.; Smith, A.M.; Hoffman, C.; Hudak, A.T.; Falkowski, M.J.; Swanson, M.E.; Gessler, P.E. Investigating the influence of LiDAR ground surface errors on the utility of derived forest inventories. *Can. J. For. Res.* **2012**, *42*, 413–422. [CrossRef]
141. Śliwiński, D.; Konieczna, A.; Roman, K. Geostatistical resampling of LiDAR-derived DEM in wide resolution range for modelling in SWAT: A case study of Zgłowiączka River (Poland). *Remote Sens.* **2022**, *14*, 1281. [CrossRef]
142. Van Leeuwen, M.; Maatern, N. Retrieval of forest structual parameters using LiDAR remote sensing. *Eur. J. For. Res.* **2010**, *129*, 749–770. [CrossRef]
143. Zhao, K.; Popescu, S.; Nelson, R. Lidar remote sensing of forest biomass: A scale-invariant estimation approach using airborne lasers. *Remote Sens. Environ.* **2009**, *113*, 182–196. [CrossRef]
144. Kaartinen, H.; Hyyppä, J.; Yu, X.; Vastaranta, M.; Hyyppä, H.; Kukko, A.; Holopainen, M.; Heipke, C.; Hirschmugl, M.; Morsdorf, F.; et al. An international comparison of individual tree detection and extraction using airborne laser scanning. *Remote Sens.* **2012**, *4*, 950–974. [CrossRef]
145. Omasa, K.; Hosoi, F.; Uenishi, T.M.; Shimizu, Y.; Akiyama, Y. Three-dimensional modeling of an urban park and trees by combined airborne and portable on-ground scanning LIDAR remote sensing. *Environ. Model. Assess.* **2008**, *13*, 473–481. [CrossRef]
146. Wang, Y.; Hyyppa, J.; Liang, X.; Kaartinen, H.; Yu, X.; Lindberg, E.; Holmgren, J.; Qin, Y.; Mallet, C. International benchmarking of the individual tree detection methods for modeling 3-D canopy structure for silviculture and forest ecology using airborne laser scanning. *IEEE Trans. Geosci. Remote Sens.* **2016**, *54*, 5011–5027. [CrossRef]
147. Li, L.; Li, D.; Zhu, H.; Li, Y. A dual growing method for the automatic extraction of individual trees from mobile laser scanning data. *ISPRS J. Photogramm. Remote Sens.* **2016**, *120*, 37–52. [CrossRef]
148. Zhang, Y.; Shao, Z. Assessing of urban vegetation biomass in combination with LiDAR and high-resolution remote sensing images. *Int. J. Remote Sens.* **2020**, *42*, 964–985. [CrossRef]
149. Santos, A.A.; Marcato Junior, J.; Araújo, M.S.; Di Martini, D.R.; Tetila, E.C.; Siqueira, H.L.; Aoki, C.; Eltner, A.; Matsubara, E.T.; Pistori, H.; et al. Assessment of CNN-based methods for individual tree detection on images captured by RGB cameras attached to UAVS. *Sensors* **2019**, *19*, 3595. [CrossRef]
150. Nezami, S.; Khoramshahi, E.; Nevalainen, O.; Honkavaara, E. Tree species classification of drone hyperspectral and RGB imagery with Deep Learning Convolutional Neural Networks. *Remote Sens.* **2020**, *12*, 1070. [CrossRef]
151. Hartling, S.; Sagan, V.; Sidike, P.; Maimaitijiang, M.; Carron, J. Urban tree species classification using a worldview-2/3 and liDAR data fusion approach and deep learning. *Sensors* **2019**, *19*, 1284. [CrossRef]
152. Lumnitz, S. Mapping Urban Trees with Deep Learning and Street-Level Imagery. Doctoral Dissertation, University of British Columbia, Vancouver, BC, Canada, 2019.
153. He, K.; Gkioxari, G.; Doll´ar, P.; Girshick, R. Mask r-cnn. In Proceedings of the 2017 IEEE International Conference on Computer Vision (ICCV), Venice, Italy, 22–29 October 2017; pp. 2961–2969.

154. Torres, D.L.; Feitosa, R.Q.; Happ, P.N.; La Rosa, L.E.C.; Junior, J.M.; Martins, J.; Bressan, P.O.; Gonçalves, W.N.; Liesenberg, V. Applying fully convolutional architectures for semantic segmentation of a single tree species in urban environment on high resolution UAV optical imagery. *Sensors* **2020**, *20*, 563. [CrossRef]
155. Yang, M.; Mou, Y.; Liu, S.; Meng, Y.; Liu, Z.; Li, P.; Xiang, W.; Zhou, X.; Peng, C. Detecting and mapping tree crowns based on convolutional neural network and Google Earth images. *Int. J. Appl. Earth Obs. Geoinf.* **2022**, *108*, 102764. [CrossRef]
156. Ocer, N.E.; Kaplan, G.; Erdem, F.; Kucuk Matci, D.; Avdan, U. Tree extraction from multi-scale UAV images using Mask R-CNN with FPN. *Remote Sens. Lett.* **2020**, *11*, 847–856. [CrossRef]
157. Sun, Y.; Li, Z.; He, H.; Guo, L.; Zhang, X.; Xin, Q. Counting trees in a subtropical mega city using the instance segmentation method. *Int. J. Appl. Earth Obs. Geoinf.* **2022**, *106*, 102662. [CrossRef]
158. Martins, J.A.C.; Nogueira, K.; Osco, L.P.; Gomes, F.D.G.; Furuya, D.E.G.; Gonçalves, W.N.; Sant'Ana, D.A.; Marques Ramos, P.A.; Liesenberg, V.; dos Santos, J.A.; et al. Semantic segmentation of tree-canopy in urban environment with pixel-wise deep learning. *Remote Sens.* **2021**, *13*, 3054. [CrossRef]
159. Xi, X.; Xia, K.; Yang, Y.; Du, X.; Feng, H. Evaluation of dimensionality reduction methods for individual tree crown delineation using instance segmentation network and UAV multispectral imagery in urban forest. *Comput. Electron. Agric.* **2021**, *191*, 106506. [CrossRef]
160. Lumnitz, S.; Devisscher, T.; Mayaud, J.R.; Radic, V.; Coops, N.C.; Griess, V.C. Mapping trees along urban street networks with deep learning and street-level imagery. *ISPRS J. Photogramm. Remote Sens.* **2021**, *175*, 144–157. [CrossRef]
161. Korznikov, K.A.; Kislov, D.E.; Altman, J.; Doležal, J.; Vozmishcheva, A.S.; Krestov, P.V. Using U-Net-Like deep convolutional neural networks for precise tree recognition in very high resolution RGB (Red, Green, Blue) satellite images. *Forests* **2021**, *12*, 66. [CrossRef]
162. Zhao, W.; Du, S.; Emery, W.J. Object-based convolutional neural network for high-resolution imagery classification. *IEEE J. Sel. Top. Appl. Earth Obs. Remote Sens.* **2017**, *10*, 3386–3396. [CrossRef]
163. Csillik, O.; Cherbini, J.; Johnson, R.; Lyons, A.; Kelly, M. Identification of citrus trees from unmanned aerial vehicle imagery using convolutional neural networks. *Drones* **2018**, *2*, 39. [CrossRef]
164. Windrim, L.; Bryson, M. Detection, segmentation, and model fitting of individual tree stems from airborne laser scanning of forests using deep learning. *Remote Sens.* **2020**, *12*, 1469. [CrossRef]
165. Iannelli, G.; Dell'Acqua, F. Extensive exposure mapping in urban areas through deep analysis of street-level pictures for floor count determination. *Urban Sci.* **2017**, *1*, 16. [CrossRef]
166. Li, X.; Zhang, C.; Li, W.; Ricard, R.; Meng, Q.; Zhang, W. Assessing street-level urban greenery using Google Street View and a modified green view index. *Urban For. Urban Green* **2015**, *14*, 675–685. [CrossRef]
167. Long, Y.; Liu, L. How green are the streets? An analysis for central areas of Chinese cities using Tencent Street View. *PLoS ONE* **2017**, *12*, e0171110. [CrossRef]
168. Richards, D.R.; Edwards, P.J. Quantifying street tree regulating ecosystem services using Google Street View. *Ecol. Indic.* **2017**, *77*, 31–40. [CrossRef]
169. Cordts, M.; Omran, M.; Mohamed, E.; Benenson, R.S.R.; Rehfeld, T.; Franke, U.; Roth, S.; Schiele, B. The cityscapes dataset for semantic urban scene understanding. In Proceedings of the 2016 IEEE Conference on Computer Vision and Pattern Recognition (CVPR), Las Vegas, NV, USA, 27–30 June 2016; pp. 3213–3223.
170. Xia, Y.; Yabuki, N.; Fukuda, T. Development of a system for assessing the quality of urban street-level greenery using street view images and deep learning. *Urban For. Urban Green* **2021**, *59*, 126995. [CrossRef]